Universal Strategy for HF-Free Facile and Rapid Synthesis of Two-dimensional MXenes as Multifunctional Energy Materials

Sin-Yi Pang,[1] Yuen-Ting Wong,[1] Shuoguo Yuan,[1] Yan Liu,[1] Ming-Kiu Tsang,[2,1] Zhibin Yang,[1] Haitao Huang[1], Wing-Tak Wong,[2] and Jianhua Hao[1,*]

[1]Department of Applied Physics, The Hong Kong Polytechnic University, Hong Kong, P. R. China

[2]Department of Applied Biology and Chemical Technology, The Hong Kong Polytechnic University, Hong Kong, P. R. China

*Corresponding author. Email: jh.hao@polyu.edu.hk

KEYWORDS: 2D materials, nano energy device, MXene, electrocatalyst, electrochemical, battery

ABSTRACT: 2D MXenes are promising for various energy-related applications such as energy storage devices and electrocatalysis of water-splitting. MXenes prepared from hydrofluoric (HF) acid etching have been widely reported. Nonetheless, the acute toxicity of HF acid impedes the large-scale fabrication of MXenes and their wide utilization in energy-related applications. It is thus greatly encouraging to explore a more innocuous protocol for MXenes synthesis. Thereby, a universal strategy based on thermal-assisted electrochemical etching route is developed to synthesize MXenes (e.g. Ti_2CT_x, Cr_2CT_x and V_2CT_x). Furthermore, the cobalt ion doped MXenes show an exceptionally-enhanced capability of hydrogen evolution reaction (HER) and oxygen evolution reaction (OER) activity, demonstrating their multifunctionalities which is comparable to the commercialized catalysts. Moreover, we successfully exploited our MXenes as cathodes for the novel aqueous rechargeable battery, with proficient retention and excellent electrical output performance. This work paves a non-toxic and HF-free route to prepare various MXenes and demonstrates practical applications of the materials.

INTRODUCTION

As an emerging class of two-dimensional (2D) material, MXenes have gained much interest because of their outstanding aptitudes for high electrical conductivity, stability, hydrophilicity and porosity, contributing to their widespread exploration in electrocatalysis and energy storage applications[1-3]. They are described by a chemical formula of $M_{n+1}X_nT_x$ (n = 1, 2 or 3; M is Ti, V or Cr; X is C or/and N; T_x is the surface functional groups of –O, –OH, –F or –Cl)[2-3]. MXenes are commonly prepared by selective chemical etching of A elements from the layered MAX materials, $M_{n+1}AX_n$ (A is the A group materials such as Al), with HF, NH_4HF_2 or a mixture of LiF/HCl[4-5]. Noted that the aqueous HF reagent is a hazardous poison with the potential for causing systemic toxicity in human body and fatality, in addition to its highly corrosive property. Hence, the direct use or *in-situ* formation of HF in these methods raises considerable safety and environmental concerns, hindering the extensive studies of MXenes. In particular, V_2C requires aggressive etching condition, 50% concentrated HF and 92 h, for production[2, 4]; while Cr_2C is unable to be prepared even via molten salt route under high temperature and pressure[6]. Accordingly, a HF-free strategy for MXenes synthesis is necessarily needed and imperative in this field. The underlying mechanism for the chemical etching is attributed to the stronger chemical active property of the M-Al bond than the M-C bond. This is intrinsically an electrochemical process involving the charge transfer from the targeted material to other species[7]. The electrochemical etching (E-etching) route has been demonstrated promising etching effectiveness on MAX precursors to selectively extract nanolaminate materials such as carbide-derived carbon (CDC) and carbon/sulfur, by tuning the etching parameters [8-10]. Moreover, surface etching of MAX phase to MXene has been achieved by using 2M hydrochloric acid at 0.6 V for 120h. It can remove the surface Al but the etching process is restricted by the formation of CDC

layers and the prolonged etching period is less favorable for large-scale production[11]. To agitate the effect of the protective CDC layers, intercalants (e.g. tetramethylammonium ion) are utilized in the synthesis, which can expand the interlayer spacing of MXenes and facilitate the etchant ions reaching the underneath un-etched MAX precursors[12]. However, the toxicity of the intercalants may also gain some concerns on the laboratory safety or health issue. In the light of these long-standing problems, we propose a thermal-assisted E-etching method to prepare HF-free MXenes (Ti_2CT_x, Cr_2CT_x and V_2CT_x) with a 3D composite electrode of carbon black (CB) additive and carbon fiber cloths (CFCs) porous substrate. The mild heating accelerates the etching on MAX materials in the presence of diluted hydrochloric acid etchant. Importantly, E-etching is commonly adopted to prepare Ti-based MXenes while reports on synthesizing other metal-based MXenes (e.g. Cr_2C and V_2C) are lacked despite their potentially sophisticated properties in electrochemical applications[2]. As a proof-of-concept, we extend our E-etching scheme to synthesize Cr_2CT_x and V_2CT_x as well, which are well known to be difficult in production [4, 6, 13]. The success in preparing these MXenes strongly indicates that our mild E-etching strategy can be a universal route for preparing various MXenes.

Despite the great challenges in their synthesis, MXenes hold strengths in their kinetic-favorable nanostructure and crystal structure. Benefiting from the oxygen adsorption favorable site[1] and the synergistic effect with electrocatalytic active promoters, MXenes have emerged as efficient electrocatalysts for oxygen evolution reaction (OER) and hydrogen evolution reaction (HER), as well as appealing electrodes for lithium ion, aluminum ion and zinc air batteries (ZAB)[1, 4, 13-14].It is noticed that zinc ion battery (ZIB) has raised much attention due to its mild neutral electrolytes and recycling costs[15]; however, its cathode requires a stable host structure and ion diffusion channel for the de/intercalation of zinc ions, which is very essential yet increases the challenges in exploring new ZIB cathode materials. To the best of our knowledge, most of the energy conversion applications were achieved with HF-etched MXenes, while MXene-based cathode with large interlayer spacing has not yet been exploited in ZIB systems. Therefore, our E-etched MXenes were explored to demonstrate their multifunctionalities in these energy conversion and storage systems. By the strict controls over the E-etching conditions, 2D MXene sheets up to 25 μm in lateral size are prepared in our synthesis route. To demonstrate the multifunctionalities of these sheets, MXenes were employed to full water-splitting catalysis and zinc ion battery system. The E-etched MXenes exhibit HER activity while their layered structure allows the intercalation of zinc ions into the MXene cathode as a ZIB. It should be emphasized that the MXene-based ZIB exhibits good retention ability (>100 cycles) and 60-folds of its initial capacity due to the activation of transition metal oxide and the water-lubricated intercalation in the oxygen-rich surface of layered MXenes. On the other hand, with good sorption affinity towards Co^{3+} ions of the E-etched MXenes, the MXene-based composite electrodes demonstrate both good HER and OER activities for full water-splitting electrocatalysis as well as a cathode for ZAB. The measured performance is comparable to the commercial OER catalysts of IrO_2 and Co^{3+}-based materials. These approaches demonstrate the potential of E-etching route as a general strategy for fabricating MXenes for multifunctional applications.

RESULTS AND DISCUSSION

Synthesis of Ti_2CT_x by E-etching with composite electrode. Ti_2CT_x was selected as the prototype to demonstrate our proposed E-etching route since Ti-based systems were prepared from a broad range of methods. The E-etching of Ti_2AlC with Cl^- etchant follows a two-stage mechanism for producing Ti_2CT_x (**Figure 1a**)[9, 11]. Owing to the weaker Ti–Al bond than Ti–C bond[9], an applied voltage removes Al atoms first from layered carbides at stage 1; and then at stage 2, both Al and Ti atoms are etched until only monolayer carbon atoms are retained. The overall E-etching reaction on Ti_2AlC is described as follows[11]:

$$Ti_2AlC + yCl^- + (2x+z)H_2O \rightarrow Ti_2C(OH)_{2x}Cl_yO_z + Al^{3+} + (x + z)H_2 + (y + 3)e^- \quad (1)$$

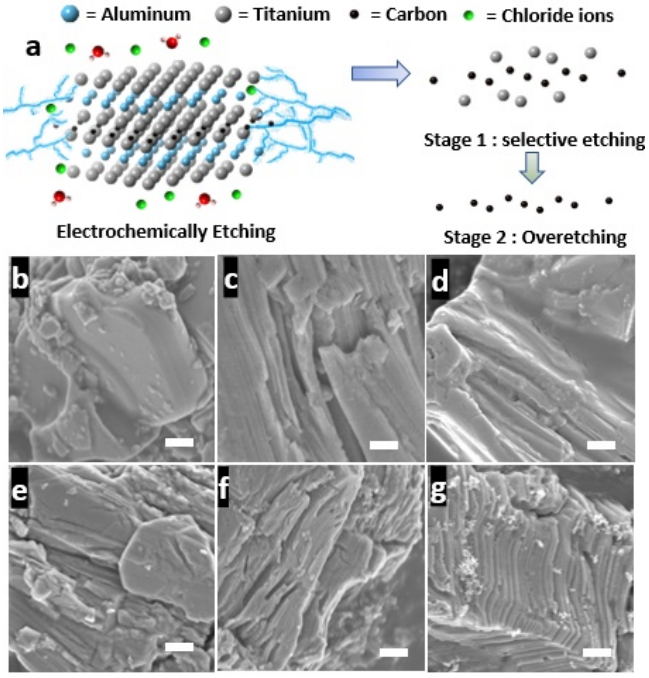

Figure 1. E-etching mechanism and morphological studies of Ti_2CT_x. (a) The proposed E-etching mechanism of Ti_2AlC in HCl electrolyte. SEM images of Ti_2CT_x produced from different E-etching conditions ([HCl]/ temperature/time/voltage). (b) un-etched Ti_2AlC, (c) 1M/25°C/9h/0.3V, (d) 1M/50°C/3h/0.3V without CB, (e) 1M/50°C/3h/0.3V, (f) 1M/50°C/6h/0.3V and (g) 1M/50°C/9h/0.3V. The scale bars are 1 μm.

First, CFCs and CB were adopted to fabricate a composite electrode with Ti_2AlC, denoted as Ti_2AlC@CB/CFC. The introduction of CB/CFC composite generates larger current across the scanning voltage (**Figure S1a**) and the composite electrode exhibits low Warburg resistance (**Figure S1b**), implying its important role in reducing ion diffusion resistance on electrolyte/electrode surface[16]. It is thus suggested that the porous CFCs and highly conductive CB con-

struct a 3D conductive network[17] of Ti_2AlC@CB/CFC to promote more efficient electrochemical reactions. The cyclic voltammogram (CV) is also important for determining a suitable range of etching voltages. Unfortunately, oxidation potentials of Al^{3+} and Ti^{3+} cannot be clearly distinguished from the broad band at 0.74 V *vs.* RHE[18]. In view of smaller oxidation potential of Al than that of Ti [9], a high voltage close to Ti^{3+} oxidation potential (at 0.74 V *vs.* RHE)[11] provokes non-selective etching (**stage 2**), associated with a wealth of etching-spots and fragments but nearly non-observable Raman signals from 0.6 V-etched Ti_2CT_x than the 0.3 V-etched one (**Figure S1c**). Hence, 0.3 V *vs*. RHE was selected as the etching voltage in order to promote more selective removal of Al atoms (**stage 1**) and prevent over-etching. Second, etching of Ti_2AlC is accelerated by gentle heating, where a greater current density of the E-etching system is obtained when the temperature is raised from 25 °C to 50 °C (**Figure S1d**). In stark contrast to smooth surface of un-etched Ti_2AlC (**Figure 1b**), the small voltage and gentle heating give rise to delamination and rougher surface on Ti_2CT_x (**Figure 1c-e**). Such a morphological change is an indication of effective E-etching, particularly for the case with thermal effect. When the etching period is extended from 3 h to 9 h, laminar structure can be successfully observed from Ti_2CT_x@1M/50°C/9h/0.3V (**Figure 1e-g**). It should be noted that CB facilitated E-etching on Ti_2AlC to give better delamination than the CB-free samples under identical synthesis condition (**Figure 1c-d**), re-assuring the importance of CB/CFC composite in the efficient etching process.

Characterizations of Ti_2CT_x. The optimized MXene displays weaker Raman signals representative for Ti_2AlC (**Figure S2a**), including the pair of vibrational peaks of non-stoichiometric titanium carbide (ω_1 and ω_3: ~ 250 and 600 cm^{-1})[19] and the vibrational peak of Al atoms in Ti_2AlC (ω_2 : ~ 420 cm^{-1})[20]. Notably, new peaks of ω_4 and ω_5 (~150 cm^{-1} and 400 cm^{-1}) are observed due to the vibration of anatase phase TiO_2 and Ti atoms, respectively[19]; while the retention of D and G broad bands indicates the presence of graphitic carbon on the sample surface[21]. **Figure S2b** shows atomic percentage of Al element was greatly reduced after the E-etching process (from 11.74 % to 0.69 %,), suggesting the effective removal of Al atoms from Ti_2AlC. Regarding XPS analysis of the MXene (**Figure S2c**), its Ti 2p spectrum shows a sharp peak for TiO (460 eV) and doublet peaks for Ti–C (464 and 455.7 eV)[14, 22]. The C–C and CH_x/C–O species are confirmed by the XPS peak at 284.5 eV along with a shoulder peak at 286.2 eV in C 1s spectrum (**Figure S2d**)[14]. The T_x-related surface features are also manifested in the XPS measurements. A sharp peak at 281 eV in **Figure S2d** is referred to C–Ti–T_x bond, possibly arising from Ti_2CO, $Ti_2C(OH)_x$ and/or Ti_2COH-H_2O. Moreover, the band in O 1s spectrum (**Figure S2e**) is composed of three peaks attributed to the surface C–Ti–$(HO)_x$ (532.0 eV), C–Ti–O_x (531.2 eV) and Ti–O (529.9 eV)[14]. It is noted that some of Al element still present in the Ti_2CT_x, featured with two prominent peaks at 73.96 and 71.47 eV due to the $2p_{3/2}$ orbit of Al^{3+} (**Figure S2f**)[23], but the Al content is low as mentioned. On the other hand, the MXene displays an obvious upshift of (002) peak from 13.02° to 9.62° (**Figure S3**), corresponding to an enlarged interlayer spacing (1.84 nm) than the pristine Ti_2AlC (1.36 nm)[24]. Noted that the 5.25° peak is due to the structural change in the crystal[25], probably from an ordered and multilayered MAX to a delaminated and swollen MXene. The SEM images in **Figure S4** reveal the ultrathin MXene sheets (with < 100 nm thickness) assemble to a flower-like architecture on Zn substrate, suggesting the successful E-etching.

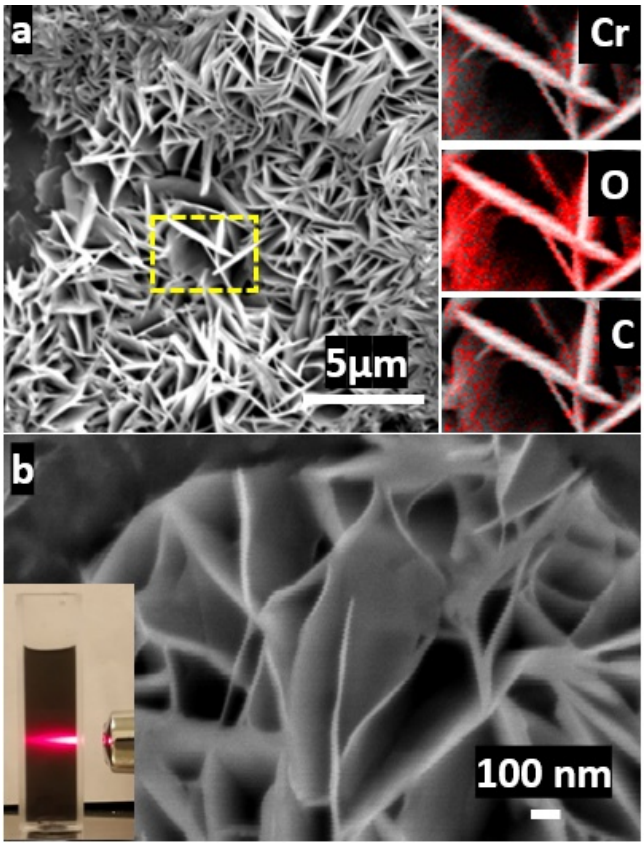

Figure 2. (a) Low-magnification and (b) high-magnification SEM images with the elemental mapping analysis of Cr_2CT_x. (Inset: digital photo of Cr_2CT_x well-dispersed in water demonstrating a clear Tyndall scattering effect).

Extended strategy to synthesize V_2CT_x and Cr_2CT_x. In fact, many compounds of MXenes are predicted as highly promising for energy-related applications. Still, there is a lack of studies on these compounds due to the great challenges in synthesis. In this regard, we attempted to explore this E-etching method as a universal way for preparing other MXenes. V_2CT_x and Cr_2CT_x were selected as representatives because they can hardly be synthesized at mild conditions and contain the same period of M as Ti. Thereby, despite its theoretically low free energy of H adsorption at equilibrium coverage[26], Cr_2CT_x is left as a theoretical compound until now. Since M-Al and M-C bonds have different strength, CV measurements were essentially conducted to determine etching voltages for each MXene. Unlike the broad CV peak of Ti_2AlC, the plateaus corresponding to Al removal can be identified, at 0.4 - 0.7 V for V_2AlC and 0.6 - 1.0 V for Cr_2AlC (**Figure S5a**). Under fixed etching conditions (i.e. 1M/50°C/9h) but various voltages, higher M/Al and M/O ratios (M = Cr, V) (**Table S1**) are resulted from 0.5 V-etched V_2CT_x and 1.0 V-etched Cr_2CT_x, respectively, indicating more selective etching at these two optimized voltages. As no reports are available for these E-etched MXenes,

we attempted to further optimize the etching voltages based on their HER performance, which concretely reveals their quality. In line with the EDX analysis, V_2CT_x and Cr_2CT_x derived from the corresponding optimized etching voltages demonstrated the best HER performance (**Figure S5b-c**). The results also imply that MAX materials with heavier M elements (Cr>V>Ti) require tougher etching conditions to synthesize MXene because of stronger M-Al bond, which is in accord with those using HF-etching[6].

To verify the successful synthesis of Cr_2CT_x and V_2CT_x, a series of characterizations were conducted. Effective Al removal on the MAX precursors is suggested based on the vanished XPS peak at 79 eV after E-etching process (**Figure S5d**). Moreover, the characteristic XPS peaks for MXenes are found from Cr_2CT_x (576 eV for chromium oxide) and V_2CT_x (523 eV for vanadium oxides), with the presence of surface functional groups (-O/-OH) (**Figure S5e-f**). Similar to the E-etched Ti_2CT_x as discussed above, the Cr_2CT_x and V_2CT_x feature an upshift of (002) XRD peak from ~13° to 9.14° and 9.29° [4], respectively, in addition to the peak at ~5.25° induced from the material delamination after etching[25] (**Figure S6**). Notably, the freshly etched MXenes are of accordion-like structure, in stark contrast to the smooth MAX materials (**Figure S7**). Upon the sonication-assisted liquid exfoliation and purification, the compact-layered MXenes separate to a wealth of sheets with a lateral size of > 1 μm and thickness of ~5 - 80 nm, which assemble to flower-like architecture as the E-etched Ti_2CT_x (**Figure 2 and S8**). The MXene flakes present essential elementals including V/Cr, C and O on their surfaces evenly. Worth-noting is that the exfoliated-Cr_2CT_x sheets are very flexible to spread onto carbon fibers (**Figure S9**), on which some large flakes (lateral size up to ~25 μm) can actually be found. This phenomenon may propose that the E-etched MXene flakes have substrate-driven architectures and benefit to form various 3D composites. Although the MXene sheets are well-dispersed in water owing to their small size and hydrophilic surface groups (**inset of Figure 2b**), the polydisperse size of MXenes can be further improved or tailored by chemically slicing or sonicating the MAX materials (~1-30 μm) to prepare desirable 3D composites. The overall product yield was estimated as ~50 % based on the weight ratio of 2D MXenes to the pristine MAX precursor. Although the produce yield can be slightly higher than that of HF-etched MXenes (~40 %)[12], some residue MAX precursors are inevitably retained in the E-etched MXenes owing to their low reactivity towards etching[4]. It should be pointed out that the product yield of our E-etching strategy can rationally be improved by recycling the sediments[12], where the conversion rate from MAX phase material to MXene can reach up to ~ 75 % because of the increased contact area with the CB/CFC 3D structure for etching. This measure is more difficult to be implemented to the case of aggressive and highly-toxic HF-etching. Hence, this E-etching method may emerge as a safer, efficient and universal way to synthesize various compounds of MXenes at large scale.

Electrocatalytic performance of MXenes for HER and the mechanism investigation. Despite the rise of MXene-based electrocatalysts for water-splitting due to their high robustness, active surface and large interspacing[14], there are limited reports about the electrocatalytic performance of MXenes synthesized from E-etching. It is found that HER occurs through the Volmer-Heyrovsky reaction rather than Tafel reaction on all the E-etched MXenes because of large Tafel slopes (**Figure S10a**) [27]. In this case, the activation energy of HER is sensitive to H coverage and H_3O^+/e^- concentration on the double layer (solid/liquid interface) [28]. These two factors closely correlate to diffusion-controlled (C_{dif}) and capacitive (C_{cap}) capacitance, while the latter is a common indicator for the electrochemical active surface area (ECSA) of a catalyst[29]. In view of such surface-dependent catalytic property, HER performance can reveal the MXene quality. Accordingly, etching effects ([HCl], temperature and time) on the Ti_2CT_x and their HER catalytic performance were examined in a three-electrode configuration.

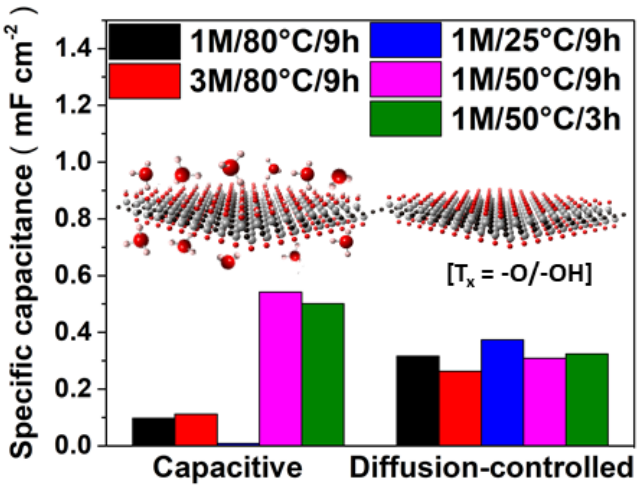

Figure 3. Bar chart showing the pseudocapacitive contribution for the various Ti_2CT_x as a mechanism study.

C_{dif} and C_{cap} were obtained from scan rate-dependent CVs of the E-etched products (**Figure S10b and Supporting formulae**) and summarized in **Figure 3** for the discussion about HER activity of E-etched Ti_2CT_x. It is found that higher [HCl] leads to enhanced surface roughness and etching depth on the Ti_2CT_x (**Figure S10c-d**), associated with slightly larger ECSA (**Figure 3**); however, η@J_s of the MXene is proportional to [HCl] (**Figure S10e**). Therefore, the best HER activity of 1M-etched Ti_2CT_x is ascribed to more effective –O/–OH surface groups present for the catalysis, as supported by greater C_{dif} (**Figure 3**) and Ti:O ratio (**Table S2**). It should be clarified that despite higher O atom%, 2M/3M-etched Ti_2CT_x contain more inactive surface TiO_2 based on a reduced Ti:O ratio (**Table S2**) but enhanced TiO_2 Raman signal at ~150 cm^{-1}(**Figure S10f**), in comparison to 1M-etched MXene. This accounts for their restrained HER activity. On the other hand, under-/ over-heating conditions (at 25°C/ 80°C) cause less superior HER catalytic performance of the Ti_2CT_x (**Figure S10g**), as a consequence of demolishing the unique structural characters of MXenes, either by inefficient etching (**Figure 1c**) or over-etching problem (**Figure 3 and S10c-d**). Accordingly, prolonged etching at the mild temperature prepares the most efficient HER catalyst, exhibiting η@J_s and Tafel slope at 570 mV and 132 mV/ decade, respectively (**Figure S10a, g**). The overpotential is high for Ti_2CT_x owing to its semi-conducting feature[26]; however

unexpectedly, the Cr_2CT_x and V_2CT_x E-etched from optimized voltages exhibit comparably large η@J_s at 540 and 610 mV, respectively (**Figure S5b-c**). Such discrepancy from the theoretic values is probably attributed to un-optimized size and etching conditions[26]. Particularly for these "hardly-etched" MXenes, higher temperature or [HCl] rationally improves etching efficiency and –O/-OH coverage on their surfaces for better catalytic properties. It is worth mentioning that their preliminary HER catalytic performance is comparable to some reported HF-etched MXenes and 2H MoS_2 (**Table S3**)[1] because of O-rich surface and the basal electrocatalytic properties[30]. In addition, the TiC_2T_x has stable catalytic ability even after 1000 cycles (**Figure S11a**). It performs better in 1 M KOH than in 1 M H_2SO_4 electrolyte (**Figure S11b**) because the HER is less favorable in the acidic environment[30]. This indicates that the E-etched MXenes have potential to serve as a cathode material in alkaline fuel cell for OER[31].

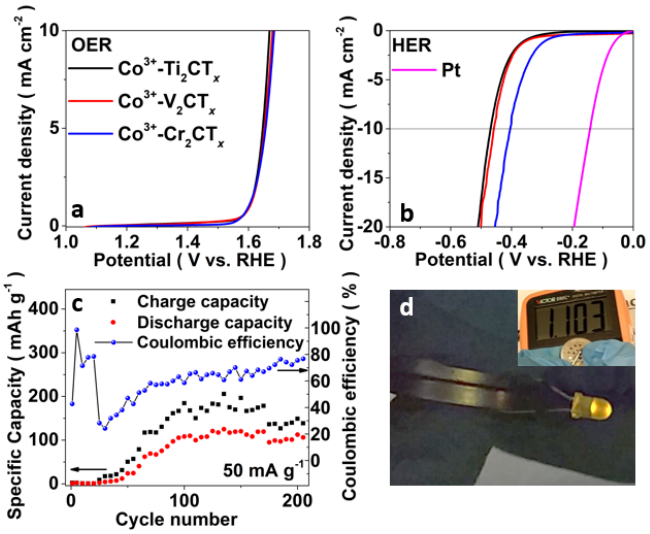

Figure 4. The demonstration of the multifunctional E-etched MXenes. The anodic-going *i*R corrected LSVs of Co^{3+}-MXenes for (a) OER and (b) HER actvity, respectively. (c)The cycling capacities and the coulombic efficiency of Cr_2CT_x cathode over 200 cycles at a current density of 50 mA g^{-1}. (d) Digital photo of a yellow LED powered up by two Co^{3+}-Cr_2CT_x-based zinc-air batteries and the inset shows the measured voltage of 1.103 V across one battery.

Metal ion doped-MXene as a bifunctional catalyst. With high robustness and affinity towards transition metals (TM) [32-33], MXenes are increasingly appealing for TM adsorption to enhance HER catalytic property[14, 27, 34] and even to endow extra functionalities for diverse applications[22, 29]. In this regard, we successfully decorated our E-etched MXenes with OER-catalytic cobalt (Co^{3+}) ions (**Figure 4a-b**), in order to achieve TM-promoted full water-splitting catalysis. The HER/OER catalytic performance of Co^{3+}-decorated MXenes (Co^{3+}-Cr_2CT_x/ V_2CT_x/ Ti_2CT_x) were tested in 1 M KOH electrolyte. The TM adsorption lowers the overpotentials for HER catalysis on all E-etched MXenes at least by 110 mV (**Table S3**), yet their performance ranking remains unchanged as the bare E-etched samples (Co^{3+}-Cr_2CT_x, 404 mV> Co^{3+}-Ti_2CT_x, 458 mV> Co^{3+}-V_2CT_x, 460 mV). In addition, **Figure S12** presents that [HCl] is positively proportional to η@J_s of the catalysts, which demonstrates the importance of Co^{3+} ions in lowering the –OH binding energy for improved HER catalysis. In stark contrast to their various HER activities, negligible difference in OER activity is identified among these Co-MXenes with η@J_s of ~1.65 V and similar reaction kinetics (**Figure 4a and S12a**). The results suggest that the OER catalytic feature is a synergistic effect of pore-rich MXenes and OER-active Co species[14, 22] but independent of the pristine MXenes. Accordingly, such OER catalytic ability is as good as many state-of-the-art OER catalysts including IrO_2 (1.690 V *vs.* RHE)[14] as well as some reported Co-based materials (**Table S3**). Noted that the Co^{3+} decoration does not alter the excellent catalytic stability of Ti_2CT_x under 1000 cycling (**Figure S11e-f**), implying the E-etched MXenes is a stable electrocatalyst for full water-splitting. Importantly, this HF-free fabrication method can produce various good-quality MXenes as an alternative to the conventional electrocatalysts, and their catalytic uses can be extended via the incorporation with other electrochemically active materials such as Ni-Fe and CoP[22, 29].

Energy storage performance of the E-etched MXenes in ZIB and ZAB. The E-etched MXenes were drop-casted onto carbon sheets as ZIB cathodes and their charging/discharging voltages were determined from individual CV measurements (**Figure S13a and S14a-b**). Moreover, galvanic charge/discharge curves for Cr_2CT_x cathode in **Figure S13b** further ensure its charging/discharging processes triggered at 1.3 V and 0.7 V respectively, indicating the average discharge voltage (0.5 V) of MXene-based ZIB , which is similar to other ZIB systems[15]. The capacities of our MXene-based ZIB were recorded over 200 cycles at a charging/discharging current density of 50 mA g^{-1}. Cr_2CT_x cathode achieves an energy density and power density down to 150 Wh kg^{-1} and 75 W kg^{-1}, together with coulombic efficiency of 77 % (**Figure 4c**); while V_2CT_x and Ti_2CT_x cathodes exhibit more inferior specific capacity and overcharged problem likely because of their less favorable electrochemical features (**Figure S14c-e**). Furthermore, the Cr_2CT_x–based ZIB has outstanding capacity retention of 98 % over 100 cycles (i.e. 100th -200th cycle, **Figure 4c**). It is ascribed to the activation effect of Cr_2O_3 formation on the MXene[35] and the water-lubrication of accessible Zn sites[15] in the first 100 cycles, in which the MXene displays an increased in capacitance and a upshifted (002) peak from 9.28° to 8.18° (**Figure S14f and S15)**. To examine the energy storage mechanism in this ZIB system, XRD patterns of the Cr_2CT_x cathode before charging and after 50 charging/discharging cycles were recorded **Figure S15**. As the device was at the 0.3 V discharging status, $ZnCr_2O_4$ were found in the MXene cathode[36], and it gives rise to new XRD peaks at 15.2°, as well as the enlarged (002) interlayer spacing of Cr_2CT_x (with an upshifted XRD peak from 8.18° to 6.48°). Notably, those new XRD features of the Cr_2CT_x are reduced while the (002) peak downshifts to 7.45° after charging to 1.7 V. Hence, it is believed that the energy storage mechanism involves intercalation of Zn^{2+} ions into the cathode[37]. This process plays important role in activating the ZIB, in which the rate capability of Cr_2CT_x is significantly increased by 60-fold with coulombic efficiency of 95 % at the discharging current density of 100 mA g^{-1} (**Figure S16a-b**). The diffusion-controlled

capacitive factor increases from 71 % to 90 % with decreasing scan rate charge, indicating Cr_2CT_x cathode is mainly controlled by diffusion process (**Figure S16c-d**). In light of the promising charge storage capability of bare E-etched MXene and Co^{3+}-promoted OER activity, Co^{3+}-Cr_2CT_x was exploited in a zinc ion and zinc-air/cobalt oxide battery as a proof-of-concept experiment. Thanks to the OER/ORR active surfactant (Co_3O_4)[38] and the layered structure, the Co^{3+}-Cr_2CT_x can serve as a ZIB/ZAB by simply changing the electrolyte (**Figure S16e-f**). It powered up a yellow light-emitting diode (LED) after charging for 500 s at a current density of 100 mA g^{-1} (**Figure 4d**), further demonstrating the practical use of the MXene-based devices for energy storage and conversion applications. Nonetheless, we believe that it is vital to enhance the ORR activity to attain a high-performance ZAB; and the optimization of structure and surface properties of MXenes can enhance Zn^{2+} ion uptake for improving the ZIB energy storage performance.

CONCLUSION

In conclusion, as a much safer and milder method than the conventional HF-etching, E-etching method with diluted HCl is developed to prepare MXene (Ti_2CT_x), whose structural and surface properties changed with various E-etching conditions. This method has been successfully extended to produce other MXenes (e.g., V_2CT_x and Cr_2CT_x), which provides an effective solution to the long-standing problem with concentrated HF involved and demonstrate its promises to be a universal way for MXene preparation. The as-synthesized MXene via the HF-free strategy can reach to 25 μm and a flower-like architecture. Moreover, the E-etched MXenes exhibited not only HER but also the capability of Co^{3+} ion adsorption to form a multifunctional catalyst for E-chem water splitting under alkaline medium. The HER (404 mV) and OER ($\eta@J_s$ = 425 mV) activities of Co^{3+}-decorated MXenes are comparable to some state-of-the-art catalysts. Also, the practical energy storage and conversion applications of Co^{3+}-MXene cathode are tested as a mode of switchable battery. The E-etched MXenes are also demonstrated for energy storage in aqueous ZIB systems and the optimized MXene exhibited a specific capacity of 100 mAh g^{-1}@50 mA g^{-1}. Therefore, this work paves a way in developing HF-free and rapid synthesis of 2D layered MXenes, which is very attractive for efficient heavy metal absorption, multifunctional electrocatalytic and energy storage applications.

ASSOCIATED CONTENT

Supporting Information.
This material is available free of charge via the Internet at http://pubs.acs.org."

Including the detailed methods, the supporting formulae, tables and figures.

AUTHOR INFORMATION

*jh.hao@polyu.edu.hk

Notes

The authors declare no competing financial interest.

ACKNOWLEDGMENT

This work was supported by the grants from Research Grants Council of Hong Kong CRF No. C7036-17W and GRF No. PolyU 153033/17P, and PolyU Grant Nos. G-UABC and 1-BBAK.

REFERENCES

(1) Seh, Z. W.; Fredrickson, K. D.; Anasori, B.; Kibsgaard, J.; Strickler, A. L.; Lukatskaya, M. R.; Gogotsi, Y.; Jaramillo, T. F.; Vojvodic, A., Two-dimensional molybdenum carbide (MXene) as an efficient electrocatalyst for hydrogen evolution. *ACS Energy Lett.* **2016**, *1*, 589-594.
(2) Anasori, B.; Lukatskaya, M. R.; Gogotsi, Y., 2D metal carbides and nitrides (MXenes) for energy storage. *Nat. Rev. Mater.* **2017**, *2*, 16098.
(3) Gao, G.; O'Mullane, A. P.; Du, A., 2D MXenes: a new family of promising catalysts for the hydrogen evolution reaction. *ACS Catal.* **2016**, *7*, 494-500.
(4)VahidMohammadi, A.; Hadjikhani, A.; Shahbazmohamadi, S.; Beidaghi, M., Two-dimensional vanadium carbide (MXene) as a high-capacity cathode material for rechargeable aluminum batteries. *ACS Nano* **2017**, *11*, 11135-11144.
(5) Mashtalir, O.; Lukatskaya, M. R.; Zhao, M. Q.; Barsoum, M. W.; Gogotsi, Y., Amine-assisted delamination of Nb_2C MXene for Li-ion energy storage devices. *Adv. Mater.* **2015**, *27*, 3501-3506.
(6) Frey, N. C.; Wang, J.; Vega Bellido, G. I. n.; Anasori, B.; Gogotsi, Y.; Shenoy, V. B., Prediction of synthesis of 2D Metal carbides and nitrides (MXenes) and their precursors with positive and unlabeled machine learning. *ACS Nano* **2019**.
(7) Srivastava, P.; Mishra, A.; Mizuseki, H.; Lee, K.-R.; Singh, A. K., Mechanistic insight into the chemical exfoliation and functionalization of Ti_3C_2 MXene. *ACS Appl. Mater. Interfaces* **2016**, *8*, 24256-24264.
(8) Zhao, M. Q.; Sedran, M.; Ling, Z.; Lukatskaya, M. R.; Mashtalir, O.; Ghidiu, M.; Dyatkin, B.; Tallman, D. J.; Djenizian, T.; Barsoum, M. W., Synthesis of carbon/sulfur nanolaminates by electrochemical extraction of titanium from Ti_2SC. *Angew. Chem. Int. Ed.* **2015**, *54*, 4810-4814.
(9) Lukatskaya, M. R.; Halim, J.; Dyatkin, B.; Naguib, M.; Buranova, Y. S.; Barsoum, M. W.; Gogotsi, Y., Room-temperature carbide-derived carbon synthesis by electrochemical etching of MAX phases. *Angew. Chem. Int. Ed.* **2014**, *53*, 4877-4880.
(10) Ortiz, G. F.; Hanzu, I.; Knauth, P.; Lavela, P.; Tirado, J. L.; Djenizian, T., TiO_2 nanotubes manufactured by anodization of Ti thin films for on-chip Li-ion 2D microbatteries. *Electrochim. Acta* **2009**, *54*, 4262-4268.
(11) Sun, W.; Shah, S.; Chen, Y.; Tan, Z.; Gao, H.; Habib, T.; Radovic, M.; Green, M., Electrochemical etching of Ti_2AlC to Ti_2CT_x (MXene) in low-concentration hydrochloric acid solution. *J. Mater. Chem. A* **2017**, *5*, 21663-21668.
(12) Yang, S.; Zhang, P.; Wang, F.; Ricciardulli, A. G.; Lohe, M. R.; Blom, P. W.; Feng, X., Fluoride-free synthesis of two-dimensional titanium carbide (MXene) using a binary aqueous system. *Angew. Chem* **2018**, *130*, 15717-15721.
(13) Naguib, M.; Halim, J.; Lu, J.; Cook, K. M.; Hultman, L.; Gogotsi, Y.; Barsoum, M. W., New two-dimensional niobium and vanadium carbides as promising materials for Li-ion batteries. *J. Am. Chem. Soc.* **2013**, *135*, 15966-15969.
(14) Zhao, L.; Dong, B.; Li, S.; Zhou, L.; Lai, L.; Wang, Z.; Zhao, S.; Han, M.; Gao, K.; Lu, M., Interdiffusion reaction-assisted hybridization of two-dimensional metal-organic frameworks and $Ti_3C_2T_x$ nanosheets for electrocatalytic oxygen evolution. *ACS Nano* **2017**, *11*, 5800-5807.

(15) Yan, M.; He, P.; Chen, Y.; Wang, S.; Wei, Q.; Zhao, K.; Xu, X.; An, Q.; Shuang, Y.; Shao, Y., Water-lubricated intercalation in $V_2O_5{\cdot}nH_2O$ for high-capacity and high-rate aqueous rechargeable zinc batteries. *Adv. Mater.* **2018**, *30*, 1703725.
(16) Yan, J.; Wei, T.; Shao, B.; Ma, F.; Fan, Z.; Zhang, M.; Zheng, C.; Shang, Y.; Qian, W.; Wei, F., Electrochemical properties of graphene nanosheet/carbon black composites as electrodes for supercapacitors. *Carbon* **2010**, *48*, 1731-1737.
(17) Yu, L.; Hu, L.; Anasori, B.; Liu, Y.-T.; Zhu, Q.; Zhang, P.; Gogotsi, Y.; Xu, B., MXene-bonded activated carbon as a flexible electrode for high-performance supercapacitors. *ACS Energy Lett.* **2018**, *3*, 1597-1603.
(18) Bao, S. J.; Li, C. M.; Zang, J. F.; Cui, X. Q.; Qiao, Y.; Guo, J., New nanostructured TiO_2 for direct electrochemistry and glucose sensor applications. *Adv. Funct. Mater.* **2008**, *18*, 591-599.
(19) Ahmed, B.; Anjum, D. H.; Hedhili, M. N.; Gogotsi, Y.; Alshareef, H. N., H_2O_2 assisted room temperature oxidation of Ti_2C MXene for Li-ion battery anodes. *Nanoscale* **2016**, *8*, 7580-7587.
(20) Spanier, J. E.; Gupta, S.; Amer, M.; Barsoum, M. W., Vibrational behavior of the $M_{n+1}AX_n$ phases from first-order Raman scattering (M= Ti, V, Cr, A= Si, X= C, N). *Phys. Rev. B* **2005**, *71*, 012103.
(21) Urbonaite, S.; Hälldahl, L.; Svensson, G., Raman spectroscopy studies of carbide derived carbons. *Carbon* **2008**, *46*, 1942-1947.
(22) Yu, M.; Zhou, S.; Wang, Z.; Zhao, J.; Qiu, J., Boosting electrocatalytic oxygen evolution by synergistically coupling layered double hydroxide with MXene. *Nano Energy* **2018**, *44*, 181-190.
(23) Wang, J.; Fan, G.; Li, F., A hybrid nanocomposite precursor route to synthesize dispersion-enhanced Ni catalysts for the selective hydrogenation of o-chloronitrobenzene. *Catal. Sci. Technol.* **2013**, *3*, 982-991.
(24) Liu, F.; Zhou, A.; Chen, J.; Jia, J.; Zhou, W.; Wang, L.; Hu, Q., Preparation of Ti_3C_2 and Ti_2C MXenes by fluoride salts etching and methane adsorptive properties. *Appl. Surf. Sci.* **2017**, *416*, 781-789.
(25) Roth, W. J.; Gil, B.; Makowski, W.; Marszalek, B.; Eliášová, P., Layer like porous materials with hierarchical structure. *Chem. Soc. Rev.* **2016**, *45*, 3400-3438.
(26) Pandey, M.; Thygesen, K. S., Two-Dimensional MXenes as catalysts for electrochemical hydrogen evolution: A computational screening study. *J. Phys. Chem. C* **2017**, *121*, 13593-13598.
(27) Ling, C.; Shi, L.; Ouyang, Y.; Chen, Q.; Wang, J., Transition metal-promoted V_2CO_2 (MXenes): A new and highly active catalyst for hydrogen evolution reaction. *Adv. Sci.* **2016**, *3*, 1600180.
(28) Zhan, C.; Naguib, M.; Lukatskaya, M.; Kent, P. R.; Gogotsi, Y.; Jiang, D.-e., Understanding the MXene pseudocapacitance. *J. Phys. Chem. Lett.* **2018**, *9*, 1223-1228.
(29) Xiu, L.; Wang, Z.; Yu, M.; Wu, X.; Qiu, J., Aggregation-Resistant 3D MXene based architecture as efficient bifunctional electrocatalyst for overall water splitting. *ACS Nano* **2018**, *12*, 8017-8028.
(30) Handoko, A. D.; Fredrickson, K. D.; Anasori, B.; Convey, K. W.; Johnson, L. R.; Gogotsi, Y.; Vojvodic, A.; Seh, Z. W., Tuning the basal plane functionalization of two-dimensional metal carbides (MXenes) to control hydrogen evolution activity. *ACS Appl. Energy Mater.* **2017**, *1*, 173-180.
(31) Tahir, M.; Pan, L.; Idrees, F.; Zhang, X.; Wang, L.; Zou, J.-J.; Wang, Z. L., Electrocatalytic oxygen evolution reaction for energy conversion and storage: A comprehensive review. *Nano Energy* **2017**, *37*, 136-157.
(32) Peng, Q.; Guo, J.; Zhang, Q.; Xiang, J.; Liu, B.; Zhou, A.; Liu, R.; Tian, Y., Unique lead adsorption behavior of activated hydroxyl group in two-dimensional titanium carbide. *J. Am. Chem. Soc.* **2014**, *136*, 4113-4116.
(33) Luo, J.; Tao, X.; Zhang, J.; Xia, Y.; Huang, H.; Zhang, L.; Gan, Y.; Liang, C.; Zhang, W., Sn^{4+} ion decorated highly conductive Ti_3C_2 MXene: promising lithium-ion anodes with enhanced volumetric capacity and cyclic performance. *ACS Nano* **2016**, *10*, 2491-2499.
(34) Wang, C.; Xie, H.; Chen, S.; Ge, B.; Liu, D.; Wu, C.; Xu, W.; Chu, W.; Babu, G.; Ajayan, P. M., Atomic cobalt covalently engineered interlayers for superior lithium-ion storage. *Adv. Mater.* **2018**, *30*, 1802525.
(35) Zeng, Y.; Lai, Z.; Han, Y.; Zhang, H.; Xie, S.; Lu, X., Oxygen-vacancy and surface modulation of ultrathin nickel cobaltite nanosheets as a high-energy cathode for advanced zn-ion batteries. *Adv. Mater.* **2018**, *30*, 1802396.
(36) Mousavi, Z.; Soofivand, F.; Esmaeili-Zare, M.; Salavati-Niasari, M.; Bagheri, S., $ZnCr_2O_4$ nanoparticles: facile synthesis, characterization, and photocatalytic properties. *Sci. Rep.* **2016**, *6*, 20071.
(37) Kundu, D.; Adams, B. D.; Duffort, V.; Vajargah, S. H.; Nazar, L. F., A high-capacity and long-life aqueous rechargeable zinc battery using a metal oxide intercalation cathode. *Nat. Energy* **2016**, *1*, 16119.
(38) Liang, Y.; Li, Y.; Wang, H.; Zhou, J.; Wang, J.; Regier, T.; Dai, H., Co_3O_4 nanocrystals on graphene as a synergistic catalyst for oxygen reduction reaction. *Nat. Mater.* **2011**, *10*, 780.

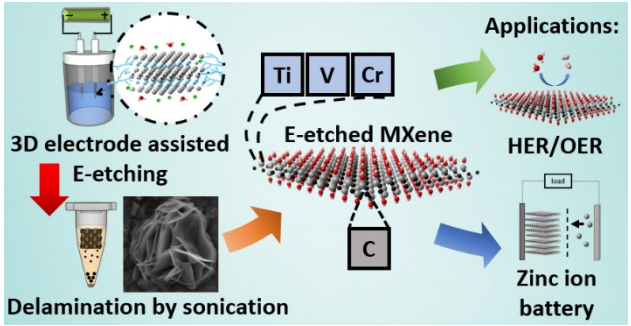

Table of Contents artwork here